JACS
JOURNAL OF THE AMERICAN CHEMICAL SOCIETY
pubs.acs.org/JACS

Article

Tunable Electrochemical Entropy through Solvent Ordering by a Supramolecular Host

Kay T. Xia, Aravindh Rajan, Yogesh Surendranath, Robert G. Bergman,* Kenneth N. Raymond,* and F. Dean Toste*

Cite This: J. Am. Chem. Soc. 2023, 145, 25463−25470

Read Online

ACCESS | Metrics & More | Article Recommendations | Supporting Information

ABSTRACT: An aqueous electrochemically controlled host−guest encapsulation system demonstrates a large and synthetically tunable redox entropy change. Electrochemical entropy is the basis for thermally regenerative electrochemical cycles (TRECs), which utilize reversible electrochemical processes with large molar entropy changes for thermogalvanic waste-heat harvesting and electrochemical cooling, among other potential applications. A supramolecular host−guest system demonstrates a molar entropy change of 4 times that of the state-of-the-art aqueous TREC electrolyte potassium ferricyanide. Upon encapsulation of a guest, water molecules that structurally resemble amorphous ice are displaced from the host cavity, leveraging a change in the degrees of freedom and ordering of the solvent rather than the solvation of the redox-active species to increase entropy. The synthetic tunability of the host allows rational optimization of the system's ΔS, showing a range of −51 to −101 cal mol^{-1} K^{-1} (−2.2 to −4.4 mV K^{-1}) depending on ligand and metal vertex modifications, demonstrating the potential for rational design of high-entropy electrolytes and a new strategy to overcome theoretical limits on ion solvation reorganization entropy.

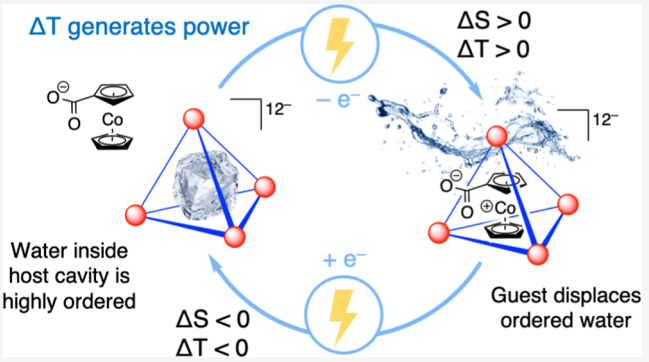

INTRODUCTION

Liquid water demonstrates many unique properties due to hydrogen-bonding networks and strong directional interactions. Confinement of water within hydrophobic molecular cavities has been observed to disrupt the structure and preferential ordering of water molecules.[1−3] Supramolecular hosts interact with encapsulated guests, including solvent molecules, through noncovalent electrostatic and steric effects, creating unique interior microenvironments divergent from bulk solution conditions.[4,5] Encapsulation of small molecules within the $[Ga_4L_6]^{12-}$ tetrahedral host[6] has long been known to be entropically driven, due to displacement of ordered solvent molecules from the host cavity.[7−11] A recent study using terahertz spectroscopy revealed that water molecules encapsulated in the host cavity are highly organized, with a structure resembling amorphous ice.[12] The encapsulation of a cationic guest molecule within the tetrahedron displaces 8−10 water molecules and desolvates the charged guest, resulting in a large systemic increase in entropy. The magnitude of this entropic gain is sensitive to the solvent conditions and the structure of the guest molecule. The modular nature of these metal−ligand coordination cage hosts enables systematic investigation of structure−activity relationships,[13−16] with the potential to gain fundamental insights into water organization and solvation entropy.

There are few existing ways to rationally tune the reaction entropy despite this property's great utility. Because of the relationship $\Delta G = \Delta H - T\Delta S$, nonzero reaction entropy forms the basis for conversion between heat (T) and free energy (ΔG). Numerous applications in energy efficiency and green technologies can be derived from systems with large and reversible reaction entropy. Phase change materials are one example of a field where a rational molecular design approach is taken to enhancing entropy, with uses in energy storage, heat harvesting, and cooling.[17,18] Thermally regenerative electrochemical cycles (TRECs) utilize a reversible redox entropy change to convert between heat and electricity, presenting a potential application of a solution-state high-entropy supramolecular electrolyte system. Engineers have employed TRECs for electrochemical heat engines and refrigerators.[19,20] The equilibrium potential of an electrochemical system has a dependence on temperature, provided that the entropy of the system is not zero (the thermogalvanic effect) (Figure 1a). In

Received: September 15, 2023
Revised: October 19, 2023
Accepted: October 23, 2023
Published: November 13, 2023

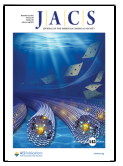

https://doi.org/10.1021/jacs.3c10145
J. Am. Chem. Soc. 2023, 145, 25463−25470

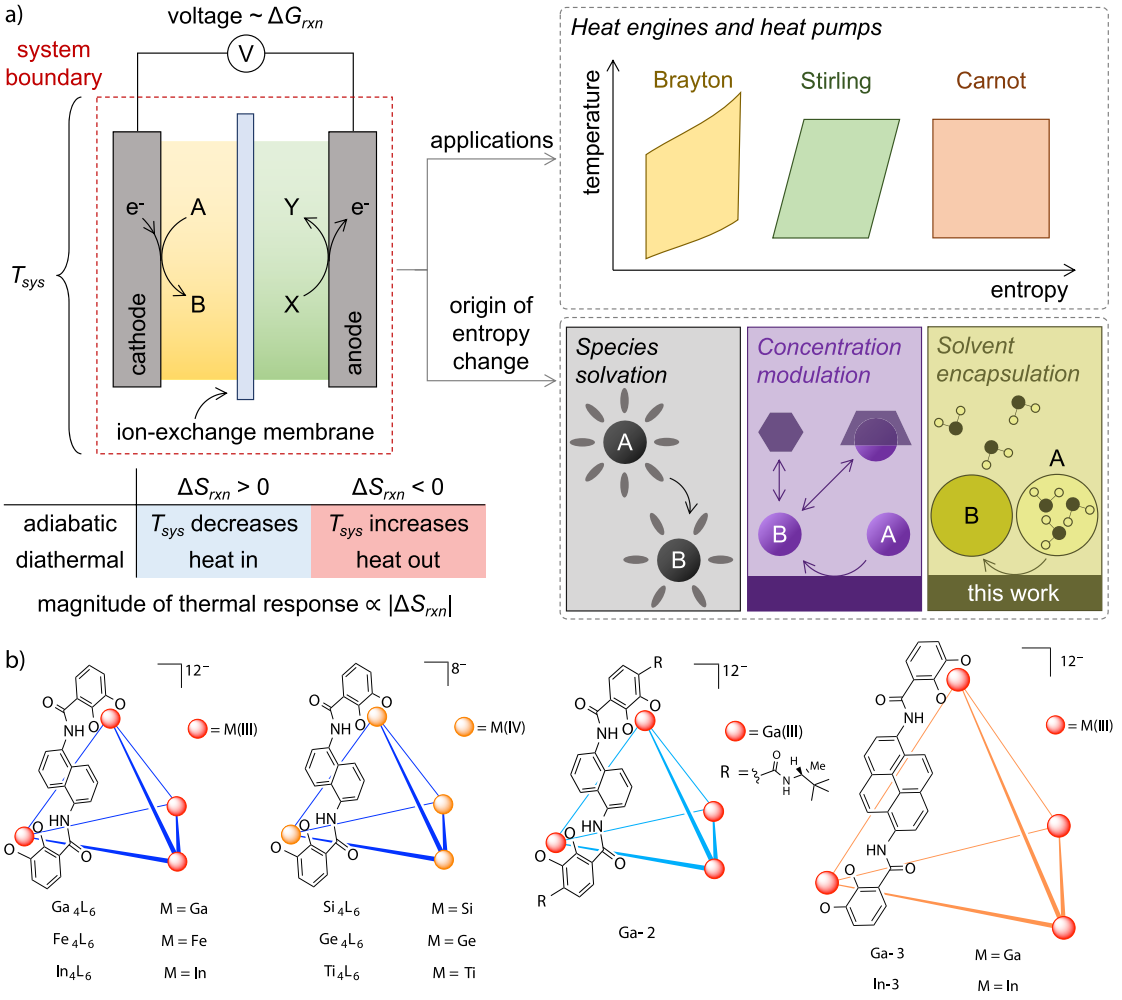

Figure 1. (a) Scheme representing the relationship between thermodynamic parameters and heat-work conversion. (b) Structural diversity of the M_4L_6 tetrahedral supramolecular host assembly. The metal centers form the vertices of the tetrahedron, and the ligands bind along the edges. For clarity, only one ligand is shown along the edge of each tetrahedron. Counterions for all hosts are K^+.

its simplest application, this relationship between the temperature and electrochemical potential enables temperature sensing. Thermogalvanic engines can also convert low-grade heat into electric current, and conversely, thermogalvanic refrigerators convert electric power to heat absorption, leading to cooling. The efficiency of these conversions is dependent on the Seebeck temperature coefficient (α), which is proportional to the molar entropy (ΔS) of the system: a larger ΔS of the redox couple leads to a larger temperature change per mole of electrons transferred. These electrochemical heat engines can be used to harvest waste heat from thermal energy generation,[21−23] and electrochemical refrigerators provide a cooling method that can avoid the use of volatile coolants,[24−26] which can contribute to atmospheric pollution (hydrofluorocarbons, currently the most common coolant in vapor compression systems, have a global warming potential of up to 2000 times that of CO_2 when leaked).[27,28] To improve the efficiency of TRECs, an electrolyte with a large and reversible entropic change is required.[29] So far, most TRECs have used simple salts as electrolytes, relying on electrochemical changes in solvation entropy, with ferri/ferrocyanide ($FCN^{4-/3-}$) being the most promising choice. Optimization experiments have been conducted,[30,31] usually involving changes in the counterion, solvent, or concentration of the electrolyte, but these salts are not amenable to synthetic design and modification. Solvation entropy is also bounded by inherent limitations, as described by the Born expression for reaction entropy,[32] leading to a fundamental bottleneck in this technology.[33]

We hypothesized that an electrochemically controlled guest encapsulation process using the M_4L_6 host would result in a system with a large and redox-controlled entropic change, which would be synthetically tunable through the structure of the host and guest. This host−guest system would represent the first of its kind in the TREC literature. The entropic change in the M_4L_6 supramolecular system reported herein relies not only on solvent reorganization but also more closely resembles a solvent phase change, resembling materials that undergo phase changes.[17,18,34−38] The entropy change arises from the large gain in degrees of freedom of the solvent molecules when released from molecular confinement rather than solely from a change in solvent organization around the redox-active species. Deriving the entropic change from solvent ordering through confinement bypasses solvation entropy limitations of non-supramolecular electrolytes, and we hypothesize that the entropic change of this system would be limited instead by the entropy of the phase transition of the solvent, which is much greater.[39] Furthermore, the M_4L_6 host has proven to be amenable to structural modifications at the metal vertices and

https://doi.org/10.1021/jacs.3c10145
J. Am. Chem. Soc. 2023, 145, 25463−25470

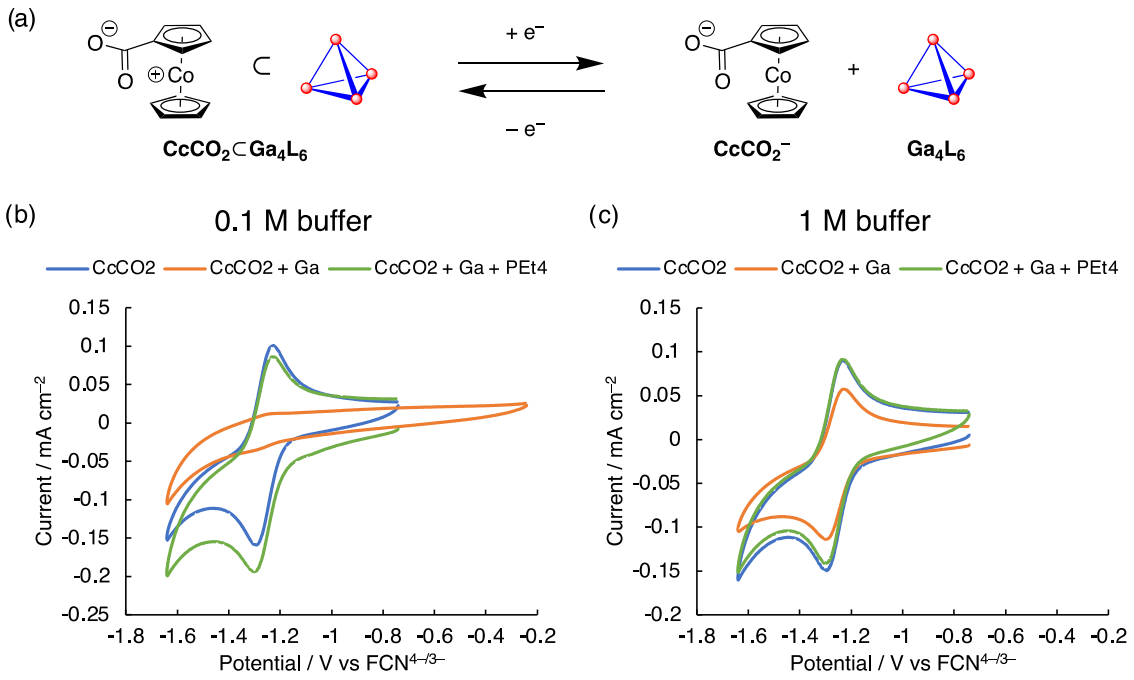

Figure 2. (a) Scheme for the electrochemical behavior of $CcCO_2$ in the presence of $[Ga_4L_6]^{12-}$. (b) Cyclic voltammogram (CV) of 2 mM $CcCO_2$ (blue), 2 mM $CcCO_2$ with 2 mM $[Ga_4L_6]^{12-}$ (orange), and 2 mM $CcCO_2$ with 2 mM $[Ga_4L_6]^{12-}$ and 2 mM PEt_4^+ (green) in 100 mM pH 12 potassium phosphate buffer in water, 100 mV s^{-1} scan rate, scanning reductively from −0.741 V vs $FCN^{4-/3-}$ for the blue and green traces, and −0.241 V vs $FCN^{4-/3-}$ for the orange trace, 1 cycle. (c) CV of 2 mM $CcCO_2$ (blue), 2 mM $CcCO_2$ with 2 mM $[Ga_4L_6]^{12-}$ (orange) and 2 mM $CcCO_2$ with 2 mM $[Ga_4L_6]^{12-}$ and 2 mM PEt_4^+ (green) in 1 M pH 12 potassium phosphate buffer in water, 100 mV/s scan rate, scanning reductively from −0.741 V vs $FCN^{4-/3-}$, 1 cycle.

of the ligand at both its linker and its end groups (Figure 1b). We envisioned that this synthetic diversification should allow for an unprecedented mechanistic exploration of encapsulation entropy and enable rational synthetic design to optimize the entropy of the system.

RESULTS AND DISCUSSION

Our initial approach drew inspiration from Fujita and co-workers' electrochemical encapsulation of ferrocene in a metal−organic cationic host.[40] Previous studies have shown $[Ga_4L_6]^{12-}$ to encapsulate cobaltocenium and decamethylcobaltocenium.[41] Due to the proximity of ferrocene's redox couple to the oxidation potential of the host's catecholate ligands,[42] we switched to cobaltocenium (Cc^+) to allow more synthetic flexibility. The redox potential of Cc/Cc^+ is over 1 V more negative than that of the catecholate ligands; therefore, structural modifications do not risk shifting the guest oxidation potential to overlap with that of the host, and the system can operate without nearing the oxidation potential of the host. Hydrocarboxycobaltocenium hexafluorophosphate ($CcCO_2HPF_6$) was selected, due to its improved solubility and slightly less negative reduction potential compared to the parent cobaltocenium (Figure 2a).[43]

In 100 mM potassium phosphate buffer in water at pH = 12, charge-neutral $CcCO_2$ displays a reversible redox couple ($E_{1/2}$ = −1.262 V vs $FCN^{4-/3-}$) (Figure 2b). When equimolar amounts of $CcCO_2$ and $[Ga_4L_6]^{12-}$ are combined, however, the redox behavior of $CcCO_2$ is seen to be significantly silenced, implying encapsulation. $CcCO_2$ (Co(III)) is overall neutrally charged and encapsulates due to hydrophobic effects. Upon addition of an excess of strongly binding guest, tetraethylphosphonium (PEt_4^+), which effectively displaces $CcCO_2$ from the host cavity (as assayed by ^1H NMR, Figure S43), the redox behavior of $CcCO_2$ returns. These data suggest the redox inhibition of $CcCO_2$ by the host.

The Frumkin effect was investigated as an explanation for this behavior. This effect, whereby the charge repulsion between the redox species and the ordering of ions in the double layer hinders electron transfer, has been observed for highly charged species, such as persulfate salts.[44] Increasing the driving force also increases the repulsion; therefore, the effect cannot be overcome by changing the electrode potential. Modifying conditions that affect the organization of the double layer, such as temperature, electrode material, electrolyte concentration, and solvent, can allow the redox species to reside within the electron transfer distance of the electrode. No change was observed when switching from a glassy carbon working electrode to a platinum working electrode (Figure S9). Increasing the buffer concentration to 1 M, however, the redox behavior of $CcCO_2$ can be observed in the presence of the host, although the peak current is smaller (Figure 2c). The diffusion coefficient extracted from the cathodic peak current at varying scan rates of $CcCO_2$ in the presence of one equivalent of $[Ga_4L_6]^{12-}$ at 1 M buffer concentration is $3.96(3) \times 10^{-7}$ cm^2 s^{-1}, compared to $5.71(4) \times 10^{-7}$ cm^2 s^{-1} in the absence of the host, implying association of $CcCO_2$ with the host, whether internally or externally, and thus moving together as a larger unit.[45] With the addition of 1.2 equiv of PEt_4^+, the diffusion coefficient is $5.09(5) \times 10^{-7}$ cm^2 s^{-1}, implying that the $CcCO_2$ is now more freely diffusing, displaced by PEt_4^+ from its association with the host.

To determine whether the observed redox peaks in 1 M buffer corresponded to $CcCO_2$ inside or outside the host cavity, the experiment was conducted with a guest with an arbitrarily slow exchange rate from the host cavity. Decamethylcobaltocenium ($Cp^*_2Co^+$) is too large to exchange

https://doi.org/10.1021/jacs.3c10145
J. Am. Chem. Soc. 2023, 145, 25463−25470

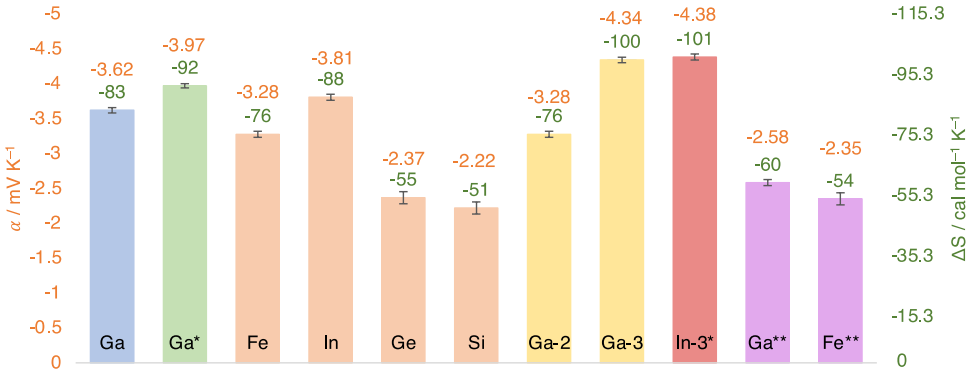

Figure 3. Redox entropy of $CcCO_2$ in the presence of various M_4L_6 hosts. Orange numbers above the bars correspond to units in mV K^{-1}, the axis on the left, and green numbers above the bars correspond to units in cal mol^{-1} K^{-1}, the axis on the right. The color of the bars is coded as follows: original system (blue), change in counterion (green), change in metal vertices of host (orange), change in ligand of the host (yellow), change in metal vertices and ligand of the host (red), at saturation concentration (purple). Unless otherwise indicated, measurements were taken with 2 mM $CcCO_2$, 2 mM M_4L_6, and 1 M pH 12 potassium phosphate buffer. * = measured with sodium phosphate buffer in place of potassium phosphate buffer. ** = measured at saturation concentration of the host: 0.1 M Ga_4L_6 or 0.1 M Fe_4L_6, respectively, with 0.1 M $CcCO_2$. Data for this graph are also provided in Table S22.

from the host cavity (the guest exchange rate is on the order of days),[46] and $[Cp^*_2Co \subset Ga_4L_6]^{11-}$ must be synthesized by templation around the $Cp^*_2Co^+$ guest. We can thus assume that $Cp^*_2Co^+$ resides exclusively within the $[Ga_4L_6]^{12-}$ cavity. No redox behavior was observed for $[Cp^*_2Co \subset Ga_4L_6]^{11-}$ (Figure S10). In contrast, the titanium-based host $[Ti_4L_6]^{8-}$ has an accessible Ti(III/IV) redox couple, and its reversible redox behavior has been measured (Figure S11). The four vertices of Ti_4L_6 are essentially electronically independent; therefore, four electrons are transferred simultaneously, and the charge of the host changes from −8 to −12. We reasoned that the host itself can access the electrode and undergo electron transfer in the double layer but only prevents electron transfer from the electrode directly to the guest, possibly due to a prohibitively high reorganization energy in the constricted cavity.

Taking these observations together, the observed redox behavior of $CcCO_2$ in the presence of $[Ga_4L_6]^{12-}$ at 1 M buffer is likely that of $CcCO_2$ associated through ion-pairing interactions to the exterior of the host. The overall neutral $CcCO_2$ binds to $[Ga_4L_6]^{12-}$ through hydrophobic effects in the naphthalene-walled cavity. It is a weakly binding guest and is observed both inside and outside the host cavity, as assessed by ^{1}H NMR spectroscopy (Figure S44). In solution, there is an equilibrium between interiorly and exteriorly associated $CcCO_2$ to $[Ga_4L_6]^{12-}$, and the concentration of $CcCO_2$ completely unassociated with the host is relatively low. At a lower ionic strength, the negative charge excess in the electrode is more poorly screened than at the higher 1 M buffer concentration, inhibiting electron transfer to the host−guest complex. As the $CcCO_2$ is associated with the host, the redox behavior observed by CV reflects a low concentration of $CcCO_2$ within electron transfer distance (Figure 2b). When the buffer concentration is raised to 1 M, the structure of the double layer now allows a higher concentration of the host to reside within electron transfer distance. By association, a higher concentration of $CcCO_2$, both interiorly and exteriorly bound to the host, is now also within electron transfer distance to the electrode, as is observed in the increased peak current by CV (Figure 2c).

We then measured the entropic change of this redox-encapsulation process. The ΔS of the encapsulation of unsubstituted cobaltocenium was found to be 62 cal mol^{-1} K^{-1} measured using ^{1}H NMR (Figure S18). The broadened signals in the NMR of $CcCO_2$ preclude measurement of its entropy of encapsulation by NMR, as these signals could not be reliably integrated. Using an electrochemical van't Hoff technique (see the Supporting Information for Method) enabled measurement of the entropy of the $CcCO_2$ Co(II/III) redox couple, as well as the entropy of the host−guest system, including both the encapsulation and redox processes (the scheme shown in Figure 2a). Two vials containing the redox solution were connected via a salt bridge, and a temperature difference was created between them by heating one side while holding the other side at a constant temperature. The difference in open-circuit potential between the solutions at different temperatures was measured and plotted against ΔT, and the slope of these points gave the Seebeck temperature coefficient in millivolts per Kelvin. This number could then be converted to ΔS in calories per mole per Kelvin through a unit conversion from millivolts to calories per mole.

The Seebeck temperature coefficient (α) of this system (2 mM $[Ga_4L_6]^{12-}$, 2 mM $CcCO_2$, 1 M pH 12 potassium phosphate buffer) was found to be −3.62(4) mV K^{-1}, which corresponds to a reaction entropy (ΔS) of 83.5(9) cal mol^{-1} K^{-1} (in comparison, α is −0.92(1) for potassium ferri/ferrocyanide). Control experiments support that encapsulation in the host is the reason for the increased ΔS, as $CcCO_2$ alone and $CcCO_2$ with the host cavity blocked by a strongly binding guest (PEt_4^+) all show significantly lower ΔS (−1.87(9) mV K^{-1} or −43(2) cal mol^{-1} K^{-1} and −2.00(4) mV K^{-1} or −46.0(9) cal mol^{-1} K^{-1}, respectively). Despite the increase in ΔS of the system in the presence of the host, a shift in $E_{1/2}$ (proportional to ΔG) is not observed in the CV (Figure 2c), although one on the order of ∼200 mV would be expected for a strongly binding guest. Enthalpy−entropy compensation effects have been observed in these host−guest systems.[11] The absence of a shift in the voltametric peak in Figure 2c upon introduction of $[Ga_4L_6]^{12-}$ implies weak host−guest binding ($K_a \sim 1$) and would be consistent with guest ion pairing to the outside of the host cavity. The large entropic value is most likely attributed to displacement of the solvent from within the host cavity, so the guest is likely to reside both inside and

https://doi.org/10.1021/jacs.3c10145
J. Am. Chem. Soc. 2023, 145, 25463−25470

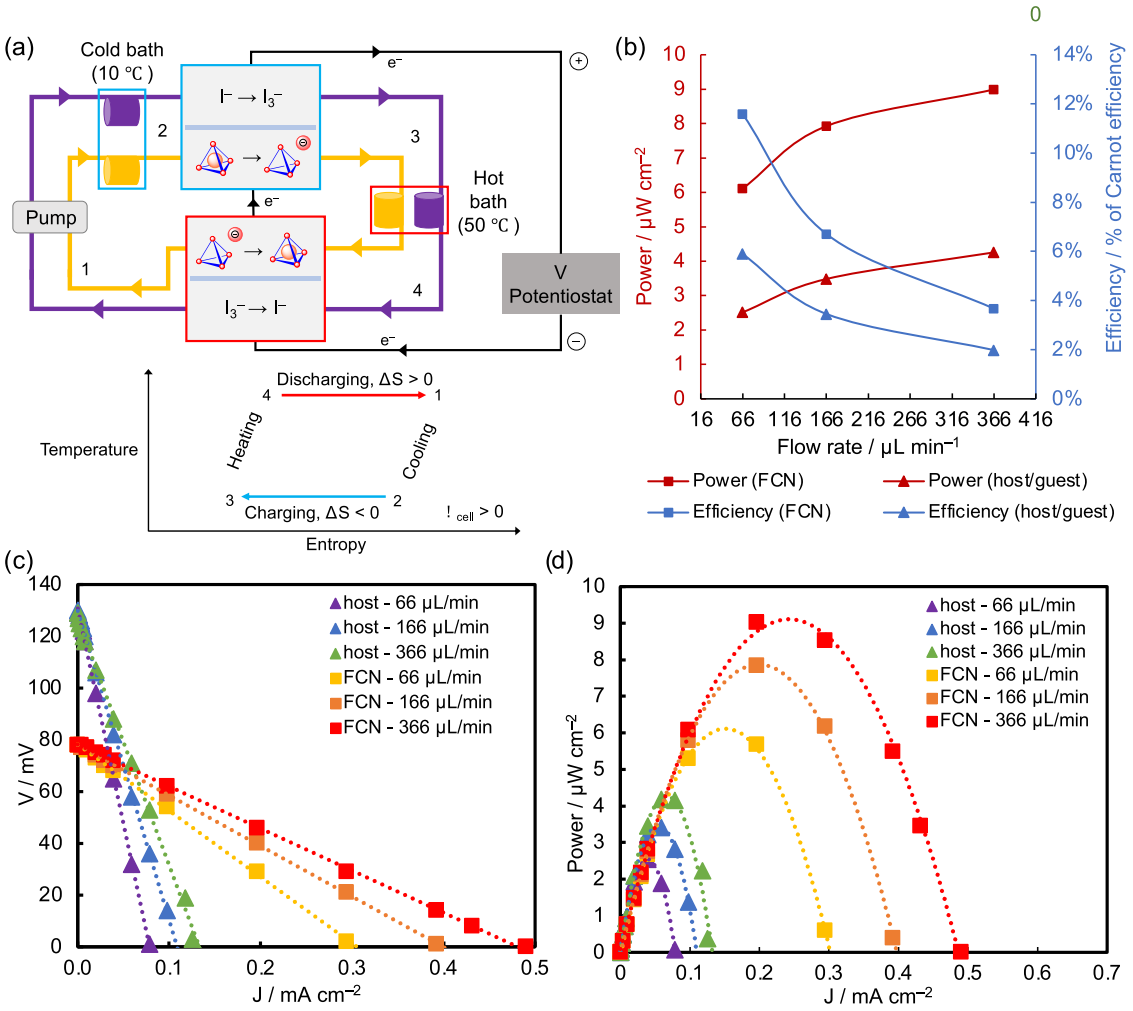

Figure 4. (a) Scheme depicting the construction of the thermogalvanic heat engine. For simplicity, the host–guest redox process is depicted with the guest encapsulated within the host, but reduction of the guest likely occurs outside the host cavity. A temperature vs entropy diagram for the cycle is shown below, with corresponding states 1–4 labeled on the device scheme. (b) Power and efficiency of the thermogalvanic heat engine at different flow rates. Data for this graph are also provided in Table S30. (c) Electrochemical potential at varying current density for the thermogalvanic heat engine at different flow rates. (d) Power at varying current density for the thermogalvanic heat engine at different flow rates.

outside of the host cavity in equilibrium. This entropic value represents a 4-fold increase versus the state-of-the-art TREC electrolyte, potassium ferricyanide.[29] Furthermore, synthetic modifications of the host system demonstrated large variations in the entropy (Figure 3). The ligand with the greatest ΔS was Ga-**3** (Figure 1), presumably due to the larger cavity size,[47] which can accommodate more water molecules that are then released upon encapsulation of the guest. The hosts with 8^- charge ($[Si_4L_6]^{8-}$ and $[Ge_4L_6]^{8-}$) showed significantly lower ΔS. Switching from potassium phosphate buffer to sodium phosphate buffer also raised ΔS, possibly due to the mixture of cations, which has been shown to have an effect on solvent organization.[31] Taking the conditions and host structural features that gave the highest ΔS, we synthesized and measured the ΔS of In-**3** in sodium phosphate buffer to be $-4.38(6)$ mV K^{-1} or $-101(1)$ cal mol^{-1} K^{-1}.

A few electrolyte systems that bear superficial similarities to the M_4L_6 host–guest system have been reported. The iodide/triiodide redox couple has been used as an electrolyte that leverages a change in the degrees of freedom of the redox species ($I_3^- \rightleftharpoons 3\ I^-$), but it does not significantly outperform ferricyanide.[48−50] A supramolecular system that uses α-cyclodextrin and iodide/triiodide has also been reported,[51] achieving $\alpha = 2.6$ mV K^{-1}. Another system has been reported in which the ferri/ferrocyanide electrolyte switches between crystalline precipitate and solution state,[52] achieving up to $\alpha = 3.73$ mV K^{-1}. Though these systems contain supramolecular host–guest chemistry and a phase change, respectively, both of these systems modulate the local concentration of the redox species at the hot and cold electrodes (either through supramolecular encapsulation or precipitation out of solution) and thereby increase the Seebeck coefficient through the relationship between potential and molar quotient described by the Nernst equation. These systems cannot generate power continuously, however, as the electrolyte must be regenerated batchwise, and generating a precipitate also risks passivating the electrode. The M_4L_6 system instead derives entropy primarily from the ordering of solvent in confinement. The M_4L_6 host–guest system represents the first system to use solvent encapsulation and release to generate an electrochemical entropic change, with the advantage of being entirely solution-state and compatible with continuously run thermogalvanic devices.

https://doi.org/10.1021/jacs.3c10145
J. Am. Chem. Soc. 2023, 145, 25463−25470

A simple thermogalvanic heat harvesting engine was constructed and tested with the host–guest system and potassium ferri/ferrocyanide, respectively, both paired with iodide/triiodide, which has a positive Seebeck coefficient (α = 0.5 mV K^{-1}) (Figure 4a).[23,24] Measurements for the host–guest system were performed at pH 12 because the hosts tend to have higher solubility at higher pH. While the solubility of most M_4L_6 hosts has been found to be less than 50 mM, the solubility of $[Ga_4L_6]^{12-}$ and $[Fe_4L_6]^{12-}$ were found to be higher. Because $[Fe_4L_6]^{12-}$ is stable to oxygen and higher temperatures, we chose to scale up the $[Fe_4L_6]^{12-}$ host–guest system for a direct comparison with the potassium ferri/ferrocyanide system at their respective saturation concentrations (for the host–guest system, measurements were performed with an aqueous solution of 0.1 M $[Fe_4L_6]^{12-}$, 0.1 M $CcCO_2HPF_6$, and 1 M pH 12 potassium phosphate buffer; for the ferri/ferrocyanide system, measurements were performed with an aqueous solution of 0.3 M $K_3Fe(CN)_6$ and 0.3 M $K_4Fe(CN)_6$). At saturation, the host–guest system demonstrated a Seebeck temperature coefficient of α = −2.35(8) mV K^{-1} (ΔS = −54(2) cal mol^{-1} K^{-1}), compared to α = −0.92(1) mV K^{-1} for potassium ferri/ferrocyanide.

The peak power for the potassium ferri/ferrocyanide system is 9 μW cm^{-2} at 4% of Carnot efficiency, matching the reported results.[23] The host–guest system achieves a higher efficiency value of 6% of Carnot efficiency at a low flow rate, though with a lower power density of 2.5 μW cm^{-2} (Figure 4b). At a higher flow rate, the peak power density rises to 4.3 μW cm^{-2}, and the efficiency drops to 2% of Carnot efficiency. This performance demonstrates the feasibility of applying a fundamental property of a supramolecular system (encapsulation entropy) to a functional device. The power density and efficiency of the host–guest system can be improved through further synthetic modifications to improve the solubility of the host. Assuming that current density scales linearly with concentration, the host–guest system can be expected to outperform potassium ferri/ferrocyanide when it achieves a concentration of over approximately 0.2 M, double its present solubility (see the Supporting Information for calculation). In future work and scale-ups of this system, synthetic design can be employed to improve other aspects as well, by replacing cobalt, gallium, and indium, for example, as the mining of these metals is known to be ethically concerning,[53−55] or by making operating conditions more benign by designing for a system closer to neutral pH to reduce corrosivity. The structural tunability of the supramolecular system engenders the possibility of engineering improvements to its properties through chemical synthesis and demonstrates the potential contribution of an approach to such projects through physical organic chemistry.

CONCLUSIONS

While the M_4L_6 tetrahedron has long been known to induce a large entropic increase upon encapsulation of a guest, this feature was until now understood as an interesting property of a supramolecular system. With this work, however, it has been shown that fundamental properties can still find new practical applications. While chemists frequently consider the energy and enthalpy of systems, we less often use molecular design to address entropic properties, and we have fewer strategies to do so. Supramolecular chemists have long performed studies to understand the fundamental properties and rules underlying noncovalent interactions, which contribute to systemic entropy changes. Supramolecular assemblies have the advantage of being adaptable to homogeneous solution-state systems, and the systems reported in this paper leverage the molecular confinement of water to demonstrate some of the largest Seebeck coefficients observed. Therefore, we identify this as a topic of interest in which synthetic chemists, materials scientists, and engineers may find fruitful collaborations. Many aspects of thermogalvanic device development cannot be addressed through chemistry research alone (for example, designing for ease of recycling or degradation at the end of the device's lifetime or considering the cost of production and modularity of the system, which could preclude adoption of these devices in low-income communities), so we urge collaboration and critical evaluation from adjacent fields, including but not limited to engineering, environmental policy and health, and energy and resources management.

ASSOCIATED CONTENT

Supporting Information

The Supporting Information is available free of charge at https://pubs.acs.org/doi/10.1021/jacs.3c10145.

General methods; synthetic methods (synthesis of all compounds, NMR van't Hoff method); electrochemical methods (experimental protocols for all electrochemical measurements, including diagrams and photographs of setups); cyclic voltammetry; diffusion coefficients; van't Hoff plots; device testing data; ^{1}H NMR spectroscopy; UV–vis spectroscopy (PDF)

AUTHOR INFORMATION

Corresponding Authors

Robert G. Bergman − *Chemical Sciences Division, Lawrence Berkeley National Laboratory, Berkeley, California 94720, United States; Department of Chemistry, University of California, Berkeley, California 94720, United States;* orcid.org/0000-0002-3105-8366; Email: rbergman@berkeley.edu

Kenneth N. Raymond − *Chemical Sciences Division, Lawrence Berkeley National Laboratory, Berkeley, California 94720, United States; Department of Chemistry, University of California, Berkeley, California 94720, United States;* orcid.org/0000-0001-6968-9801; Email: raymond@socrates.berkeley.edu

F. Dean Toste − *Chemical Sciences Division, Lawrence Berkeley National Laboratory, Berkeley, California 94720, United States; Department of Chemistry, University of California, Berkeley, California 94720, United States;* orcid.org/0000-0001-8018-2198; Email: fdtoste@berkeley.edu

Authors

Kay T. Xia − *Chemical Sciences Division, Lawrence Berkeley National Laboratory, Berkeley, California 94720, United States; Department of Chemistry, University of California, Berkeley, California 94720, United States*

Aravindh Rajan − *Palo Alto Research Center, Palo Alto, California 94304, United States*

Yogesh Surendranath − *Department of Chemistry, Massachusetts Institute of Technology, Cambridge, Massachusetts 02139, United States;* orcid.org/0000-0003-1016-3420

Complete contact information is available at:

https://pubs.acs.org/10.1021/jacs.3c10145

Author Contributions

All authors were involved in the writing and revision of this article and have given approval to the final version of the manuscript.

Notes

The authors declare no competing financial interest.

■ ACKNOWLEDGMENTS

This research was supported by the Director, Office of Science, Office of Basic Energy Sciences, and the Division of Chemical Sciences, Geosciences, and Bioscience of the U.S. Department of Energy at Lawrence Berkeley National Laboratory (Grant DE-AC02-05CH11231). The authors thank Dr. Hasan Celik and UC Berkeley's NMR facility in the College of Chemistry (CoC-NMR) for spectroscopic assistance. Instruments in the CoC-NMR are supported in part by National Institute of Health grant S10OD024998. The authors thank Alexandra Grigoropoulos and Professor Ting Xu for lending assistance and their differential scanning calorimeter for measuring heat capacity data. The authors would like to thank Andrew L. Smith for lending assistance with the use of python.

■ REFERENCES

(1) Tunuguntla, R. H.; Henley, R. Y.; Yao, Y. C.; Pham, T. A.; Wanunu, M.; Noy, A. Enhanced Water Permeability and Tunable Ion Selectivity in Subnanometer Carbon Nanotube Porins. *Science* **2017**, *357* (6383), 792−796, DOI: 10.1126/science.aan2438.

(2) Hummer, G.; Rasaiah, J. C.; Noworyta, J. P. Water Conduction through the Hydrophobic Channel of a Carbon Nanotube. *Nature* **2001**, *414* (6860), 188−190.

(3) Itoh, Y.; Chen, S.; Hirahara, R.; Konda, T.; Aoki, T.; Ueda, T.; Shimada, I.; Cannon, J. J.; Shao, C.; Shiomi, J.; Tabata, K. V.; Noji, H.; Sato, K.; Aida, T. Ultrafast Water Permeation through Nanochannels with a Densely Fluorous Interior Surface. *Science* **2022**, *376* (6594), 738−743.

(4) Brown, C. J.; Toste, F. D.; Bergman, R. G.; Raymond, K. N. Supramolecular Catalysis in Metal-Ligand Cluster Hosts. *Chem. Rev.* **2015**, *115* (9), 3012−3035.

(5) Morimoto, M.; Bierschenk, S. M.; Xia, K. T.; Bergman, R. G.; Raymond, K. N.; Toste, F. D. Advances in Supramolecular Host-Mediated Reactivity. *Nat. Catal.* **2020**, *3* (12), 969−984.

(6) Hong, C. M.; Bergman, R. G.; Raymond, K. N.; Toste, F. D. Self-Assembled Tetrahedral Hosts as Supramolecular Catalysts. *Acc. Chem. Res.* **2018**, *51* (10), 2447−2455.

(7) Biros, S. M.; Bergman, R. G.; Raymond, K. N. The Hydrophobic Effect Drives the Recognition of Hydrocarbons by an Anionic Metal-Ligand Cluster. *J. Am. Chem. Soc.* **2007**, *129* (40), 12094−12095.

(8) Sgarlata, C.; Mugridge, J. S.; Pluth, M. D.; Zito, V.; Arena, G.; Raymond, K. N. Different and Often Opposing Forces Drive the Encapsulation and Multiple Exterior Binding of Charged Guests to a M4L6 Supramolecular Vessel in Water. *Chem. - Eur. J.* **2017**, *23* (66), 16813−16818.

(9) Sgarlata, C.; Mugridge, J. S.; Pluth, M. D.; Tiedemann, B. E. F.; Zito, V.; Arena, G.; Raymond, K. N. External and Internal Guest Binding of a Highly Charged Supramolecular Host in Water: Deconvoluting the Very Different Thermodynamics. *J. Am. Chem. Soc.* **2010**, *132* (3), 1005−1009.

(10) Sgarlata, C.; Raymond, K. N. Untangling the Diverse Interior and Multiple Exterior Guest Interactions of a Supramolecular Host by the Simultaneous Analysis of Complementary Observables. *Anal. Chem.* **2016**, *88* (13), 6923−6929.

(11) Leung, D. H.; Bergman, R. G.; Raymond, K. N. Enthalpy-Entropy Compensation Reveals Solvent Reorganization as a Driving Force for Supramolecular Encapsulation in Water. *J. Am. Chem. Soc.* **2008**, *130* (9), 2798−2805.

(12) Sebastiani, F.; Bender, T. A.; Pezzotti, S.; Li, W. L.; Schwaab, G.; Bergman, R. G.; Raymond, K. N.; Dean Toste, F.; Head-Gordon, T.; Havenith, M. An Isolated Water Droplet in the Aqueous Solution of a Supramolecular Tetrahedral Cage. *Proc. Natl. Acad. Sci. U.S.A.* **2020**, *117* (52), 32954−32961.

(13) Hong, C. M.; Kaphan, D. M.; Bergman, R. G.; Raymond, K. N.; Toste, F. D. Conformational Selection as the Mechanism of Guest Binding in a Flexible Supramolecular Host. *J. Am. Chem. Soc.* **2017**, *139* (23), 8013−8021.

(14) Hong, C. M.; Morimoto, M.; Kapustin, E. A.; Alzakhem, N.; Bergman, R. G.; Raymond, K. N.; Toste, F. D. Deconvoluting the Role of Charge in a Supramolecular Catalyst. *J. Am. Chem. Soc.* **2018**, *140* (21), 6591−6595.

(15) Nguyen, Q. N. N.; Xia, K. T.; Zhang, Y.; Chen, N.; Morimoto, M.; Pei, X.; Ha, Y.; Guo, J.; Yang, W.; Wang, L. P.; Bergman, R. G.; Raymond, K. N.; Toste, F. D.; Tantillo, D. J. Source of Rate Acceleration for Carbocation Cyclization in Biomimetic Supramolecular Cages. *J. Am. Chem. Soc.* **2022**, *144* (25), 11413−11424.

(16) Bierschenk, S. M.; Pan, J. Y.; Settineri, N. S.; Warzok, U.; Bergman, R. G.; Raymond, K. N.; Toste, F. D. Impact of Host Flexibility on Selectivity in a Supramolecular Host-Catalyzed Enantioselective Aza-Darzens Reaction. *J. Am. Chem. Soc.* **2022**, *144* (25), 11425−11433.

(17) Seo, J.; McGillicuddy, R. D.; Slavney, A. H.; Zhang, S.; Ukani, R.; Yakovenko, A. A.; Zheng, S. L.; Mason, J. A. Colossal Barocaloric Effects with Ultralow Hysteresis in Two-Dimensional Metal−Halide Perovskites. *Nat. Commun.* **2022**, *13* (1), No. 2536, DOI: 10.1038/s41467-022-29800-9.

(18) Matuszek, K.; Kar, M.; Pringle, J. M.; MacFarlane, D. R. Phase Change Materials for Renewable Energy Storage Applications. *Chem. Rev.* **2023**, *123* (1), 491−514.

(19) Bell, L. E. Cooling, Heating, Generating Power, and Recovering Waste Heat with Thermoelectric Systems. *Science* **2008**, *321* (5895), 1457−1461.

(20) Disalvo, F. J. Thermoelectric Cooling and Power Generation. *Science* **1999**, *285* (5428), 703−706.

(21) Poletayev, A. D.; McKay, I. S.; Chueh, W. C.; Majumdar, A. Continuous Electrochemical Heat Engines. *Energy Environ. Sci.* **2018**, *11* (10), 2964−2971.

(22) Zhang, H.; Zhang, F.; Yu, J.; Zhou, M.; Luo, W.; Lee, Y. M.; Si, M.; Wang, Q. Redox Targeting-Based Thermally Regenerative Electrochemical Cycle Flow Cell for Enhanced Low-Grade Heat Harnessing. *Adv. Mater.* **2021**, *33* (5), No. 2006234, DOI: 10.1002/adma.202006234.

(23) Qian, X.; Shin, J.; Tu, Y.; Zhang, J. H.; Chen, G. Thermally Regenerative Electrochemically Cycled Flow Batteries with PH Neutral Electrolytes for Harvesting Low-Grade Heat. *Phys. Chem. Chem. Phys.* **2021**, *23* (39), 22501−22514.

(24) Rajan, A.; McKay, I. S.; Yee, S. K. Continuous Electrochemical Refrigeration Based on the Brayton Cycle. *Nat. Energy* **2022**, *7* (4), 320−328.

(25) Lilley, D.; Prasher, R. Ionocaloric Refrigeration Cycle, Supplementary Information. *Science* **2022**, *378*, 1344−1348.

(26) Rajan, A.; Yee, S. K. System Dynamics and Metrics of an Electrochemical Refrigerator Based on the Brayton Cycle. *Cell Rep. Phys. Sci.* **2022**, *3* (3), No. 100774.

(27) Velders, G. J. M.; Ravishankara, A. R.; Miller, M. K.; Molina, M. J.; Alcamo, J.; Daniel, J. S.; Fahey, D. W.; Montzka, S. A.; Reimann, S. Preserving Montreal Protocol Climate Benefits by Limiting HFCs. *Science* **2012**, *335*, 922−923.

(28) Velders, G. J. M.; Fahey, D. W.; Daniel, J. S.; McFarland, M.; Andersen, S. O. The Large Contribution of Projected HFC Emissions to Future Climate Forcing. *Proc. Natl. Acad. Sci. U.S.A.* **2009**, *106* (27), 10949−10954.

(29) Rajan, A.; McKay, I. S.; Yee, S. K. Electrolyte Engineering Can Improve Electrochemical Heat Engine and Refrigeration Efficiency. *Trends Chem.* **2022**, *4* (3), 172−174.

(30) Gao, C.; Liu, Y.; Chen, B.; Yun, J.; Feng, E.; Kim, Y.; Kim, M.; Choi, A.; Lee, H. W.; Lee, S. W. Efficient Low-Grade Heat Harvesting Enabled by Tuning the Hydration Entropy in an Electrochemical System. *Adv. Mater.* **2021**, *33* (13), No. 2004717.
(31) Buckingham, M. A.; Hammoud, S.; Li, H.; Beale, C. J.; Sengel, J. T.; Aldous, L. A Fundamental Study of the Thermoelectrochemistry of Ferricyanide/Ferrocyanide: Cation, Concentration, Ratio, and Heterogeneous and Homogeneous Electrocatalysis Effects in Thermogalvanic Cells. *Sustainable Energy Fuels* **2020**, *4* (7), 3388−3399.
(32) Hupp, J. T.; Weaver, M. J. Solvent, Ligand, and Ionic Charge Effects on Reaction Entropies for Simple Transition-Metal Redox Couples. *Inorg. Chem.* **1984**, *23* (22), 3639−3644.
(33) Buckingham, M. A.; Laws, K.; Li, H.; Kuang, Y.; Aldous, L. Thermogalvanic Cells Demonstrate Inherent Physiochemical Limitations in Redox-Active Electrolytes at Water-in-Salt Concentrations. *Cell Rep. Phys. Sci.* **2021**, *2* (8), No. 100510.
(34) Umeyama, D.; Horike, S.; Inukai, M.; Itakura, T.; Kitagawa, S. Reversible Solid-to-Liquid Phase Transition of Coordination Polymer Crystals. *J. Am. Chem. Soc.* **2015**, *137* (2), 864−870.
(35) Slavney, A. H.; Kim, H. K.; Tao, S.; Liu, M.; Billinge, S. J. L.; Mason, J. A. Liquid and Glass Phases of an Alkylguanidinium Sulfonate Hydrogen-Bonded Organic Framework. *J. Am. Chem. Soc.* **2022**, *144* (25), 11064−11068.
(36) Bennett, T. D.; Horike, S. Liquid, Glass and Amorphous Solid States of Coordination Polymers and Metal−Organic Frameworks. *Nat. Rev. Mater.* **2018**, *3* (11), 431−440.
(37) Dannenfelser, R. M.; Yalkowsky, S. H. Estimation of Entropy of Melting from Molecular Structure: A Non-Group Contribution Method. *Ind. Eng. Chem. Res.* **1996**, *35* (4), 1483−1486.
(38) Wei, J. Molecular Symmetry, Rotational Entropy, and Elevated Melting Points. *Ind. Eng. Chem. Res.* **1999**, *38*, 5019−5027.
(39) Giauque, W. F.; Stout, J. W. The Entropy of Water and the Third Law of Thermodynamics. The Heat Capacity of Ice from 15 to 273 K. *J. Am. Chem. Soc.* **1936**, *58*, 1144−1150.
(40) Sun, W. Y.; Kusukawa, T.; Fujita, M. Electrochemically Driven Clathration/Declathration of Ferrocene and Its Derivatives by a Nanometer-Sized Coordination Cage. *J. Am. Chem. Soc.* **2002**, *124* (39), 11570−11571.
(41) Pluth, M. D.; Johnson, D. W.; Szigethy, G.; Davis, A. V.; Teat, S. J.; Oliver, A. G.; Bergman, R. G.; Raymond, K. N. Structural Consequences of Anionic Host-Cationic Guest Interactions in a Supramolecular Assembly. *Inorg. Chem.* **2009**, *48* (1), 111−120.
(42) Dalton, D. M.; Ellis, S. R.; Nichols, E. M.; Mathies, R. A.; Toste, F. D.; Bergman, R. G.; Raymond, K. N. Supramolecular Ga4L6 12- Cage Photosensitizes 1,3-Rearrangement of Encapsulated Guest via Photoinduced Electron Transfer. *J. Am. Chem. Soc.* **2015**, *137* (32), 10128−10131, DOI: 10.1021/jacs.5b06317.
(43) Vanicek, S.; Kopacka, H.; Wurst, K.; Müller, T.; Schottenberger, H.; Bildstein, B. Chemoselective, Practical Synthesis of Cobaltocenium Carboxylic Acid Hexafluorophosphate. *Organometallics* **2014**, *33* (5), 1152−1156.
(44) Bard, A. J.; Faulkner, L. R.Double-Layer Effects on Electrode Reaction Rates. In *Electrochemical Methods: Fundamentals and Applications*; Wiley, 2001; pp 571−575.
(45) Pluth, M. D.; Tiedemann, B. E. F.; Van Halbeek, H.; Nunlist, R.; Raymond, K. N. Diffusion of a Highly Charged Supramolecular Assembly: Direct Observation of Ion Association in Water. *Inorg. Chem.* **2008**, *47* (5), 1411−1413.
(46) Davis, A. V.; Raymond, K. N. The Big Squeeze: Guest Exchange in an M4L6 Supramolecular Host. *J. Am. Chem. Soc.* **2005**, *127* (21), 7912−7919.
(47) Johnson, D. W.; Raymond, K. N. The Self-Assembly of a [Ga4L6]12- Tetrahedral Cluster Thermodynamically Driven by Host-Guest Interactions. *Inorg. Chem.* **2001**, *40* (20), 5157−5161.
(48) Kim, K.; Kang, J.; Lee, H. Hybrid Thermoelectrochemical and Concentration Cells for Harvesting Low-Grade Waste Heat. *Chem. Eng. J.* **2021**, *426*, No. 131797.
(49) Duan, J.; Yu, B.; Liu, K.; Li, J.; Yang, P.; Xie, W.; Xue, G.; Liu, R.; Wang, H.; Zhou, J. P-N Conversion in Thermogalvanic Cells Induced by Thermo-Sensitive Nanogels for Body Heat Harvesting. *Nano Energy* **2019**, *57*, 473−479.
(50) Abraham, T. J.; MacFarlane, D. R.; Pringle, J. M. Seebeck Coefficients in Ionic Liquids -Prospects for Thermo-Electrochemical Cells. *Chem. Commun.* **2011**, *47*, 6260−6262.
(51) Zhou, H.; Yamada, T.; Kimizuka, N. Supramolecular Thermo-Electrochemical Cells: Enhanced Thermoelectric Performance by Host-Guest Complexation and Salt-Induced Crystallization. *J. Am. Chem. Soc.* **2016**, *138*, 10502−10507.
(52) Yu, B.; Duan, J.; Cong, H.; Xie, W.; Liu, R.; Zhuang, X.; Wang, H.; Qi, B.; Xu, M.; Wang, Z. L.; Zhou, J. Thermosensitive Crystallization-Boosted Liquid Thermocells for Low-Grade Heat Harvesting. *Science* **2020**, *370* (6514), 342−346.
(53) Sovacool, B. K. The Precarious Political Economy of Cobalt: Balancing Prosperity, Poverty, and Brutality in Artisanal and Industrial Mining in the Democratic Republic of the Congo. *Extr. Ind. Soc.* **2019**, *6* (3), 915−939.
(54) Fu, X.; Beatty, D. N.; Gaustad, G. G.; Ceder, G.; Roth, R.; Kirchain, R. E.; Bustamante, M.; Babbitt, C.; Olivetti, E. A. Perspectives on Cobalt Supply through 2030 in the Face of Changing Demand. *Environ. Sci. Technol.* **2020**, *54* (5), 2985−2993.
(55) White, S. J. O.; Shine, J. P. Exposure Potential and Health Impacts of Indium and Gallium, Metals Critical to Emerging Electronics and Energy Technologies. *Curr. Environ. Health Rep.* **2016**, *3* (4), 459−467.

https://doi.org/10.1021/jacs.3c10145
J. Am. Chem. Soc. 2023, 145, 25463−25470